Complex Singularities Tracking Method for PDEs

Vincenzo Sciacca

University of Palermo

Workshop on
"Hamiltonian PDEs: analitical and numerical methods"
Trieste – June 22–24, 2009

Plan:

- PART I: A review of the tracking singularities method.

Plan:

- PART I: A review of the tracking singularities method.
- PART II: Applications to $1D$ equations:
  - Camassa–Holm equation.
  - De Gasperi–Procesi equation.
  - b–family equations.

Tracking a . . .
Zero viscosity . . .
Pade . . .
Home Page
Title Page
Page 2 of 58
Go Back
Full Screen
Close
Quit

Plan:

- PART I: A review of the tracking singularities method.
- PART II: Applications to $1D$ equations:
  - Camassa–Holm equation.
  - De Gasperi–Procesi equation.
  - b–family equations.
- PART III: Zero Viscosity Limit of Navier–Stokes:
  - Prandtl's equations.
  - The Van Dommelen and Shen's singularity.
  - Navier Stokes results.
  - The Comparison between NS and Prandtl's solutions.

Plan:

- PART I: A review of the tracking singularities method.
- PART II: Applications to $1D$ equations:
  - Camassa–Holm equation.
  - De Gasperi–Procesi equation.
  - b–family equations.
- PART III: Zero Viscosity Limit of Navier–Stokes:
  - Prandtl's equations.
  - The Van Dommelen and Shen's singularity.
  - Navier Stokes results.
  - The Comparison between NS and Prandtl's solutions.
- PART IV: Conclusions

Tracking a . . .
Zero viscosity . . .
Pade . . .
Home Page
Title Page
Page 2 of 58
Go Back
Full Screen
Close
Quit

A Review: Burger's equation

$$\begin{aligned} u_t + uu_x &= 0, \qquad x \in [0, 2\pi]\,, \quad t \in [0, 1[\\ u(x, t=0) &= u_0(x) = \sin(x), \\ u(0, t) &= u(2\pi, t). \end{aligned}$$

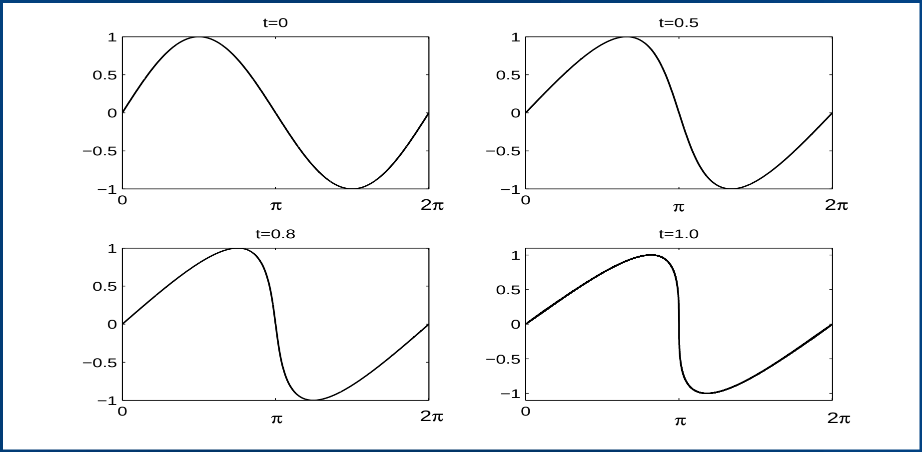

What does the Fourier–spectrum say?

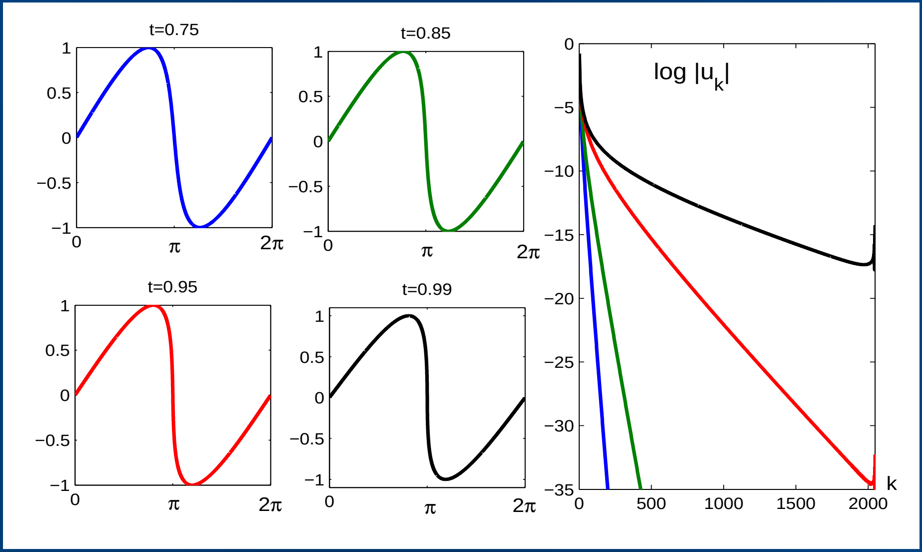

1. Tracking a singularity in the complex plane

If an analytic function

$$u(Z) = \sum_{k=0}^{\infty} a_k Z^k = (1 - Z/Z_*)^{\alpha} r(Z) + a(Z)$$

has an algebraic singularity of type α at the complex location Z_*, with

$$r(Z) = \sum_{n=0}^{\infty} b_n (1 - Z/Z_*)^n$$

then the asymptotic behavior of its Taylor coefficients is given by (Darboux Theorem):

$$a_k \sim \sum_{n=0}^{\infty} \frac{(-1)^n b_n Z_*^{n-k} \Gamma(k - \alpha - n)}{k! \Gamma(-\alpha - n)}$$

The leading term is simply

$$a_k \sim b_0 k^{-(1+\alpha)} Z_*^{-k}.$$

If $Z = exp(-iz)$, $Z_* = exp(-i(x^* + i\delta))$ and $a_k = \hat{u}_k$, then the spectrum has the following (Laplace formula) asymptotic (in k) behavior:

$$\hat{u}_k \sim C|k|^{-(1+\alpha)} \exp(-\delta k) \exp(ix^* k).$$

The rate of the exponential decay of the spectrum δ gives the distance of the singularity from the real axes.

The time t_s at which $\delta(t_s) = 0$ gives the exact time of the development of the singularity.

The estimate of x^* and α gives, respectively, the real location x^* and the algebraic type of the singularity.

The rate of the exponential decay of the spectrum δ gives the distance of the singularity from the real axes.

The time t_s at which $\delta(t_s) = 0$ gives the exact time of the development of the singularity.

The estimate of x^* and α gives, respectively, the real location x^* and the algebraic type of the singularity.
The picture behind the idea of the singularity tracking method is to complexify the spatial variable

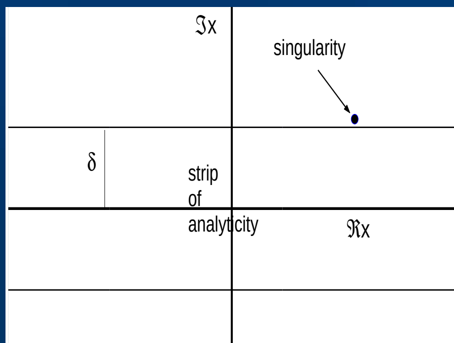

i.e. a singularity does not comes out of the blue, but sits in the complex plane, maybe headed to hit the real axis. When the singularity hits the real axis the singularity shows up in the real world as a blow up (of the solution or of the derivative depends on the algebraic character of the complex singularity).
Evaluating the exponential rate of decay of the spectrum of the solution one knows the distance δ of the singularity from the real axis.

$$\log |\hat{u}_k| \sim C - (1 + \alpha) \log(k) - \delta k$$

The method was introduced in '83 by Sulem, Sulem and H.Frisch. Their goal was the issue of the global in time regularity of the Euler equations.
Lack of computational power postponed for decades the possibility of tackling such a problem.
A more subtle issue is the fact that when the singularity approaches the real axis exponentially slow then the method can run out of steam.
However if there is a reasonable confidence that an equation develop a singularity, tracing the complex singularity has become a powerful method to follow and characterize the whole process.

- Vortex sheets:
  Shelley J. Fluid. Mech., 1992
  Cowley, Baker, and Tanveer J. Fluid. Mech., 1999
- Hele–Shaw flows:
  Goldstein, Pesci, and Shelley, Physics of Fluids, 1998
- Thin–Jets:
  Pugh and Shelley, Comm. Pure Appl. Math.1998

Tracking a . . .
Zero viscosity . . .
Pade . . .
Home Page
Title Page

Go Back
Full Screen
Close
Quit

The method was introduced in '83 by Sulem, Sulem and H.Frisch. Their goal was the issue of the global in time regularity of the Euler equations.
Lack of computational power postponed for decades the possibility of tackling such a problem.
A more subtle issue is the fact that when the singularity approaches the real axis exponentially slow then the method can run out of steam.
However if there is a reasonable confidence that an equation develop a singularity, tracing the complex singularity has become a powerful method to follow and characterize the whole process.

- Vortex sheets:
  Shelley J. Fluid. Mech., 1992
  Cowley, Baker, and Tanveer J. Fluid. Mech., 1999

- Hele–Shaw flows:
  Goldstein, Pesci, and Shelley, Physics of Fluids, 1998

- Thin–Jets:
  Pugh and Shelley, Comm. Pure Appl. Math.1998

- Complex 3D Euler with swirl:
  Caflisch Physica D, 1993
  Caflisch and Siegel, Methods Appl. Anal. 2004

- Formation of a complex singularity in 2D Euler:
  Matsumoto, Bec, U.Frisch Fluid. Dynam. Res. 2005
  Pauls, Matsumoto, Bec, U.Frisch Physica D 2006

- For a review and perspectives see:
  U.Frisch, Matsumoto and Bec, J. Statist. Phys. 2003
  Pauls and Frisch J. Statist. Phys. 2007.

Tracking complex singularity: Burger's equation

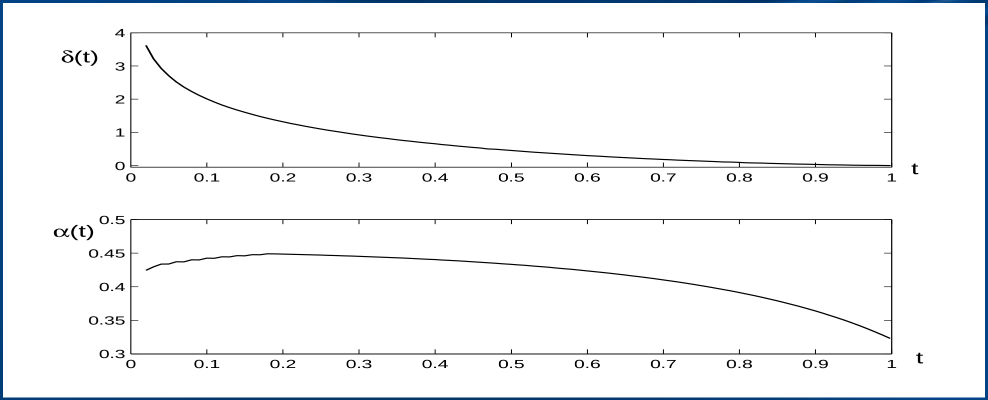

Tracking complex singularity: analytic result

In the sequel we shall be dealing with functions that are analytic in the complex variable x. We hence introduce the strip in the complex plane.

$$D(\rho) = \{x \in \mathbb{C} \ : \Im x \in (-\rho, \rho)\} \ .$$

The L^2 integration is performed along the following path:

$$\Gamma(b) = \{x \in \mathbb{C} \ : \Im x = b\} \ .$$

- $H^{0,\rho}$ is the set of all complex functions $f(x)$ such that
  - f is analytic in $D(\rho)$;
  - $f \in L^2(\Gamma(\Im x))$ for $\Im x \in (-\rho, \rho)$,; i.e. if $\Im x$ is inside $(-\rho, \rho)$, then $f(\Re x + i\Im x)$ is a square integrable function of $\Re x$;
  - $|f|_\rho = \sup_{\Im x \in (-\rho,\rho)} \|f(\cdot + i\Im x)\|_{L^2(\Gamma(\Im x))} < \infty$.
- $H^{k,\rho}$ is the set of all complex functions $f(x)$ such that
  - $\partial_x^j f \in H^{0,\rho}$ for $0 \le j \le k$;
  - $\|f\|_{k,\rho} \equiv \sum_{0 \le j \le k} |\partial_x^j f|_\rho < \infty$.

This norm is equivalent to:

$$\|f\|_{k,\rho} = \left[\int e^{2\rho|\xi|}(1 + |\xi|^2)^k \, |\hat{f}(\xi)|^2 \, d\xi\right]^{1/2} \ .$$

We now state the ACK Theorem in the form given by Safonov. Consider the problem:

$$u + F(t, u). \tag{1}$$

Theorem[ACK]
Suppose that $\exists R > 0$, $\rho_0 > 0$, and $\beta_0 > 0$ such that if $0 < t \le \rho_0/\beta_0$, the following properties hold:

(a) $\forall\, 0 < \rho' < \rho \le \rho_0$ *and* $\forall u$ *s.t.* $\{u \in X_\rho : \sup\limits_{0\le t\le T} |u(t)|_\rho \le R\}$ *the map*
$F(t,u) : [0,T] \mapsto X_{\rho'}$ *is continuous.*

(b) $\forall\, 0 < \rho < \rho_0$ *the function* $F(t,0) : [0, \rho_0/\beta_0] \mapsto \{u \in X_\rho : \sup\limits_{0\le t\le T} |u(t)|_\rho \le R\}$ *is continuous and*

$$|F(t,0)|_\rho \le R_0 < R\ .$$

(c) $\forall 0 < \rho' < \rho(s) < \rho_0$ *and* $\forall\ u$ *and* $w \in \{u \in X_\rho : \sup\limits_{0\le t\le T} |u(t)|_{\rho-\beta_0 t} \le R\}$,

$$|F(t,u) - F(t,w)|_{\rho'} \le C \int_0^t ds \left(\frac{|u-w|_{\rho(s)}}{\rho(s)-\rho'} \right).$$

Then $\exists \beta > \beta_0$ such that $\forall 0 < \rho < \rho_0$ Eq. (1) has a unique solution $u(t) \in X_\rho$ with $t \in [0, (\rho_0 - \rho)/\beta]$; moreover $\sup\limits_{\rho<\rho_0-\beta t} |u(t)|_\rho \le R$.

Under this point of view the ACK is just an analytic tool that allows to bound the speed at which the singularity travels in the complex plane.

Camassa–Holm equation: analytic results

$$u_t - u_{xxt} + 3uu_x = 2u_x u_{xx} + uu_{xxx}$$

We write the Camassa—Holm in a form suitable for the application of the ACK Theorem:

$$u_t + uu_x = -\frac{ik}{1+k^2}\left(u^2 + \frac{1}{2}u_x^2\right),$$

where k is the dual Fourier variable of x.
With an integration in time one gets $u = F(t, u)$ where:

$$F(t,u) \equiv u_0 - \int_0^t dt' \left[uu_x + \frac{ik}{1+k^2}\left(u^2 + \frac{1}{2}u_x^2\right)\right]$$

Theorem[Lombardo,Sammartino and S. 04]
Let $u_0 \in H^{1,\rho_0}$ be the initial datum of the Camassa–Holm equation. Then there exists $\beta > 0$ such that for any ρ with $0 < \rho < \rho_0$ there exists a unique continuously differentiable (w.r.t. time) solution u of the Camassa–Holm equation with the following property:

- $u(\cdot, t) \in H^{1,\rho}$ *and* $\partial_t u(\cdot, t) \in H^{1,\rho}$ *when* $t \in \left[0, \frac{\rho_0 - \rho}{\beta}\right]$.

Theorem[Lombardo,Sammartino and S. 04]
Suppose the initial datum of the Camassa–Holm equation satisfy $u_0 \in H^{r,\rho}$ with $r > 3/2$, $|u_0|_{L^1} < \infty$, $u_0 - \partial_{xx}u_0 \geq 0$ (or ≤ 0). Then the unique solution $u(x,t)$ belongs to the Gevrey class of index 1 globally in time.

Camassa–Holm equation: numerical results

$$u_t + uu_x = -\frac{ik}{1+k^2}\left(u^2 + \frac{u_x^2}{2}\right) \; ,$$

This means that, if one defines:

$$F_k(u) = -\left[\widehat{(uu_x)}_k + \frac{ik}{1+k^2}\left(\widehat{(u^2)}_k + \frac{1}{2}\widehat{(u_x^2)}_k\right)\right] \; ,$$

the dynamics of the k-th Fourier mode of u is ruled by:$\partial_t u_k = F_k(u)$. Dividing the time interval $[0, T]$ in N sub-intervals of size $\Delta t = T/N$, we write the approximation:

$$u(x, n\Delta t) \approx \sum_{k=-K/2}^{k=K/2} u_k^n e^{ikx} \; .$$

We solve the ODE's system using an explicit Runge–Kutta method of the 4–th order. The numerical scheme therefore is:

$$u_k^{n+1} = u_k^n + \frac{\Delta t}{6}\left(\Gamma_k^1 + 2\Gamma_k^2 + 2\Gamma_k^3 + \Gamma_k^4\right) \; ,$$

where $\Gamma_k^i = F_k(V^i)$ $i = 1, 2, 3, 4$, with:

$$V_k^1 = u_k^n \, , \quad V_k^2 = V_k^1 + \frac{\Delta t}{2}\Gamma_k^1 \, , \quad V_k^3 = V_k^2 + \frac{\Delta t}{2}\Gamma_k^2 \, , \quad V_k^4 = V_k^3 + \Delta t \Gamma_k^3 \, .$$

The scheme is initialized by $u_k^0 = h_k$, where h_k being the coefficients in the Fourier expansion of the initial data $h(x)$.

Camassa–Holm equation I: $h(x) = \sin(x)$

We first consider the initial datum $h(x) = \sin(x)$. Given that the integral of the datum on $[0, 2\pi]$ is zero, this datum develops singularity in finite time.

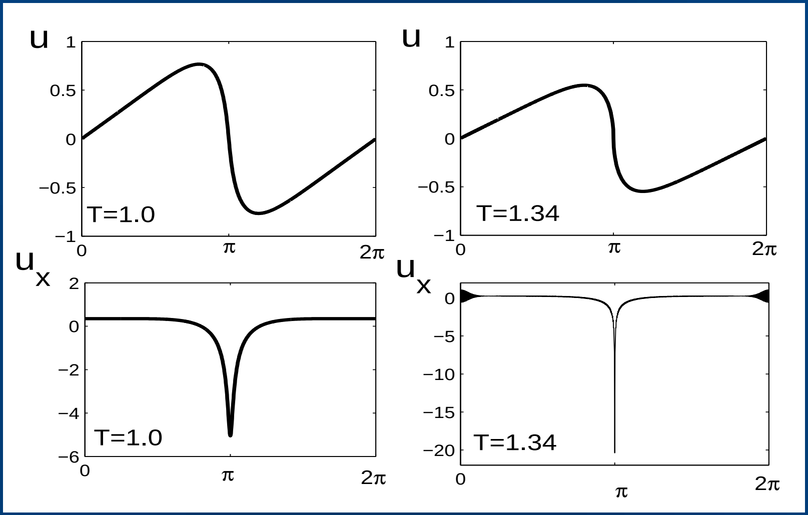

The CH solution with $h(x) = \sin(x)$. In the top two figures the solution before the singularity and at the singularity time. In the bottom figures we show the derivative of the solution.

The exponential and the algebraic decay of the spectrum.

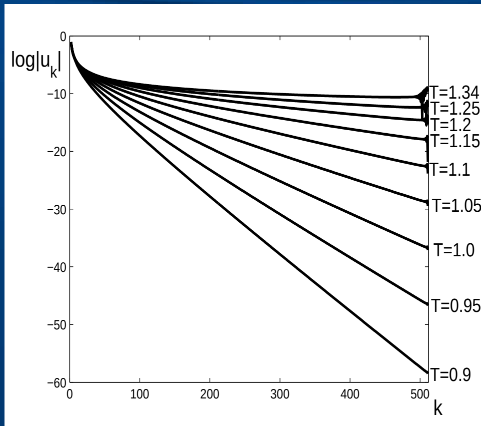

The behavior of log $|u_k|$ at different times.

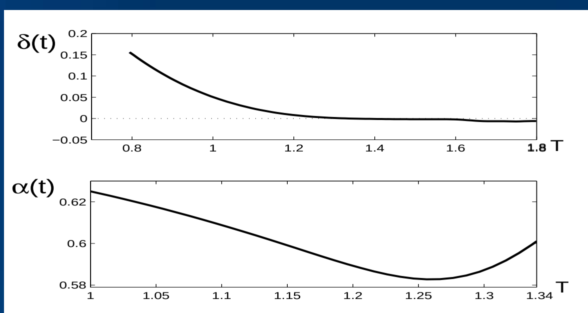

The width of the analyticity strip shrinks to zero at $t \approx 1.34$. At the singularity the solution behaves like $(x - x^*)^\alpha$ with $\alpha \approx 0.58$.

Camassa–Holm equation II: $h(x) = 1 + \sin(x)$

The condition on the initial datum $(1 - \partial_{xx})h > 0$, together with the regularity condition $h \in H^s$ $s > 3/2$, ensures the long time regularity of the solution. The initial datum $h(x) = 1 + \sin(x)$ violates this condition and it is a candidate to singularity formation.

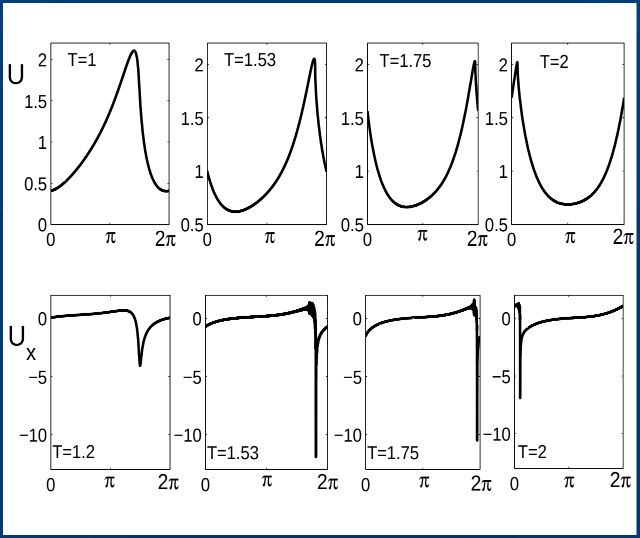

The formation of a peaked singularity. The solution seems to have a blow–up in the derivative. We have tried to follow the solution after the singularity time: the "peak" seems to move at speed approximately equal to its height $c \approx 2$.

The exponential and the algebraic decay of the spectrum.

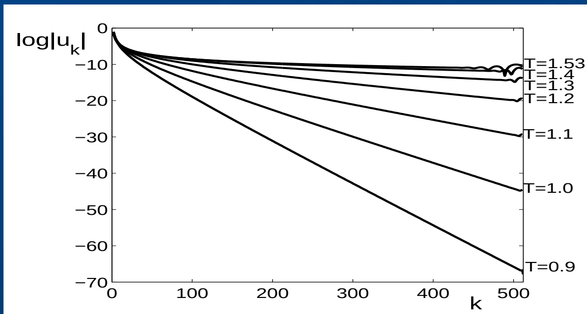

In the above figures one can follow the formation of the singularity as the shrinking to zero of the strip of analyticity.

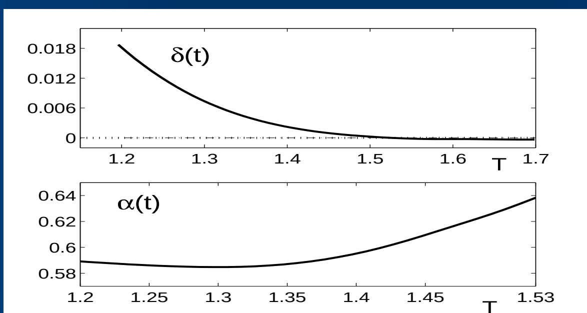

The singularity time is therefore estimated as $t_c \approx 1.53$. At the singularity time the solution behaves like $(x - x^*)^\alpha$ with $\alpha \approx 2/3$.

The oscillatory behavior of the spectrum.

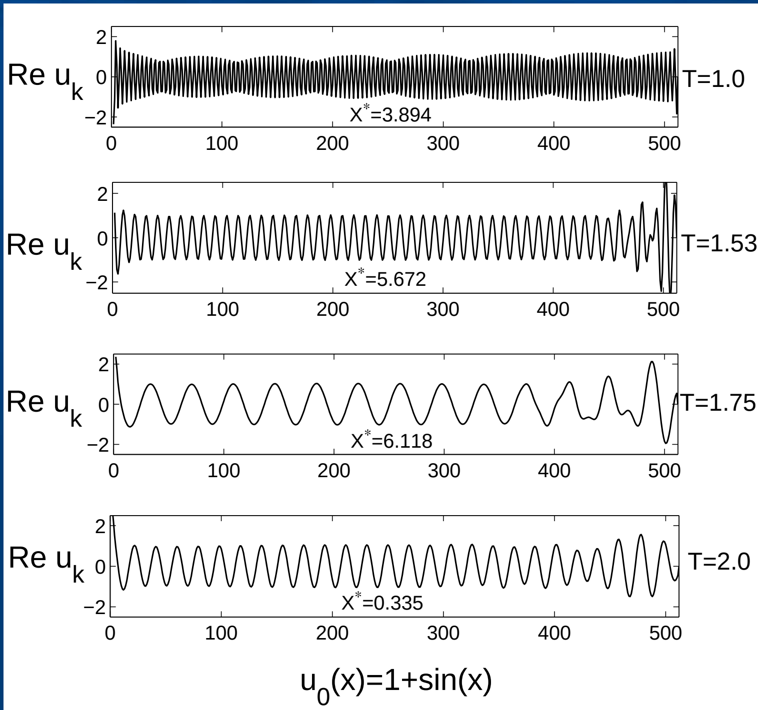

We show the behavior of the real part of the spectrum (cleared up from both the exponential and algebraic decay) at different times. The imaginary part has the same character.

b–family equations: analytic results

We apply the ACK theorem to the b–family equations (Holm & Stanley 01) to prove the short time existence of analytic solution. First of all we write the b–family equation in a form suitable for the applicatin of the ACK theorem. It is easy to see that the b–family equation can be written in the following form:

$$(1-\partial_x^2)(u_t+uu_x) = (b-3)u_x u_{xx} - buu_x = -\partial_x\left(\frac{b}{2}u^2 + \frac{3-b}{2}u_x^2\right),$$

and finally in the pseudodifferential form

$$u_t + uu_x = -A^{-2}\left(\frac{b}{2}u^2 + \frac{3-b}{2}u_x^2\right)_x,$$

where we denote by $A^2 = (1-\partial_x^2)$. Finally, with an integration in time one obtain

$$u = F(u,t), \qquad \text{with}$$

$$F(u,t) = u_0 - \int_0^t \left[uu_x + A^{-2}\left(\frac{b}{2}u^2 + \frac{3-b}{2}u_x^2\right)_x\right] dt'.$$

Theorem[Coclite and S. 09]

Let $1 \leq b \leq 3$ and let the initial data for the b–family $u_0 \in H^{1,\rho_0}$. Then there exists $\beta > 0$ such that for any ρ, with $0 < \rho < \rho_0$, there exists a unique continuously differentiable w.r.t. time solution u of the b–family equation with the following propertiy:

- $u(\cdot, t) \in H^{1,\rho}$ *and* $\partial_t u(\cdot, t) \in H^{1,\rho}$, *when* $t \in \left[0, \frac{\rho_0 - \rho}{\beta}\right]$.

Theorem[Coclite and S. 09]

Let $1 \leq b \leq 3$ and $A^2 = (1 - \partial_x^2)$. Let $u_0 \in D(A^r e^{\rho_0 A})$, with $r > 3/2$, $\rho_0 > 0$ and $m_0 = u_0 - u_{0xx}$ does not change sign. Then the unique solution u of the b–family equation lies in Gevrey class of index 1 globally in time.

Tracking a . . .
Zero viscosity . . .
Pade . . .
Home Page
Title Page
Go Back
Full Screen
Close
Quit

b–family equations: numerical results

Let us consider in this section the b–family equation in the spatial domain $[0, 2\pi]$, with periodic boundary conditions, and we solve this equation using Fourier spectral method. We use the b-family equation written in pseudodifferential form

$$u_t + uu_x = -\frac{ik}{1+k^2}\left(\frac{b}{2}u^2 + \frac{3-b}{2}u_x^2\right),$$

where now k is the dual Fourier variable of x. Then the dynamics of the kth Fourier mode of u is described by the following ODE

$$\partial_t \hat{u}_k = -\left[\widehat{(uu_x)}_k + \frac{ik}{1+k^2}\left(\frac{b}{2}\widehat{(u^2)}_k + \frac{3-b}{2}\widehat{(u_x^2)}_k\right)\right].$$

Dividing the time interval $[0, T]$ in N sub–intervals of size $\Delta t = T/N$, we approximate the solution u as

$$u(x, n\Delta t) \approx \sum_{k=-K/2}^{K/2} \hat{u}_k^n e^{ikx};$$

and we solve the system of ODE using explicit Runge–Kutta method of the 4th order with initial conditions given by

$$\hat{u}_k^0 = \hat{h}_k,$$

with $\hat{h}_k$ the Fourier coefficients of the initial data $u(x, 0) = h(x)$.

b–family equations I: $h(x) = \sin(x)$

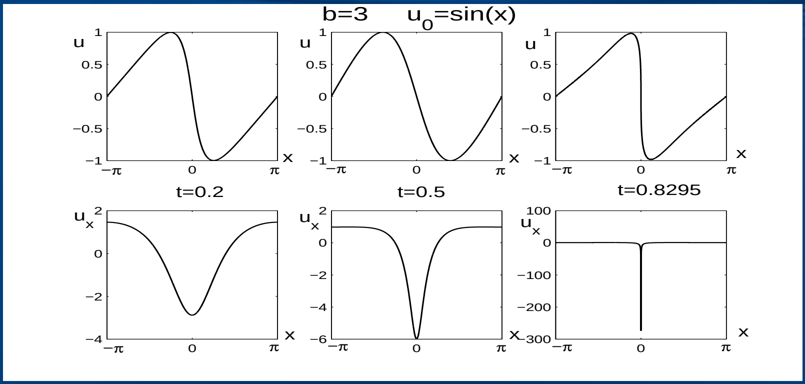

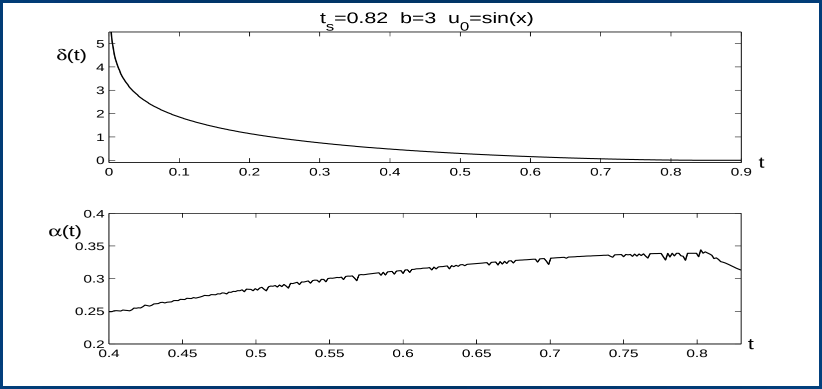

The singularity times and the type of singularities for differents values of b.

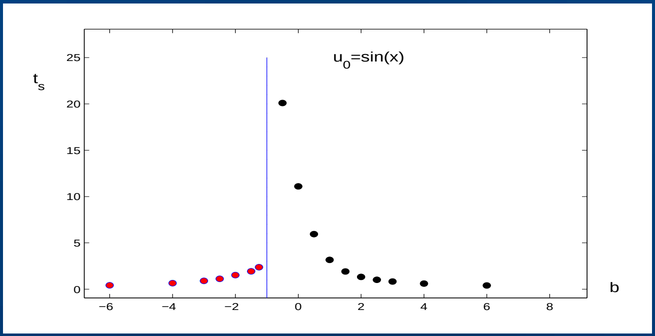

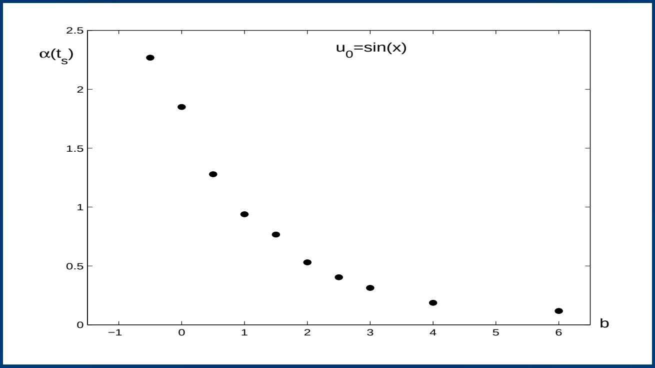

b–family equations I: $h(x) = 1 + \sin(x)$

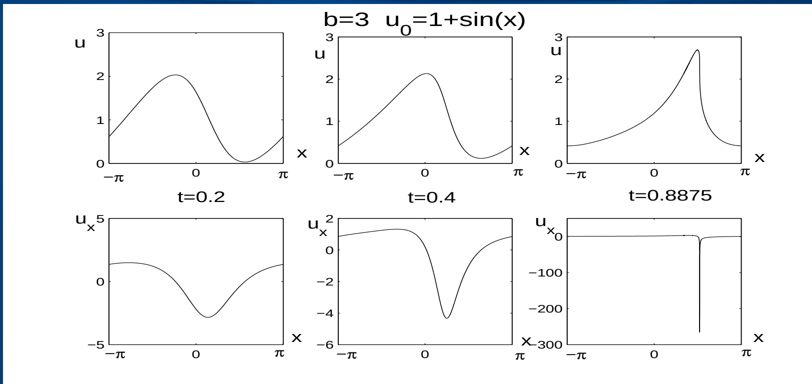

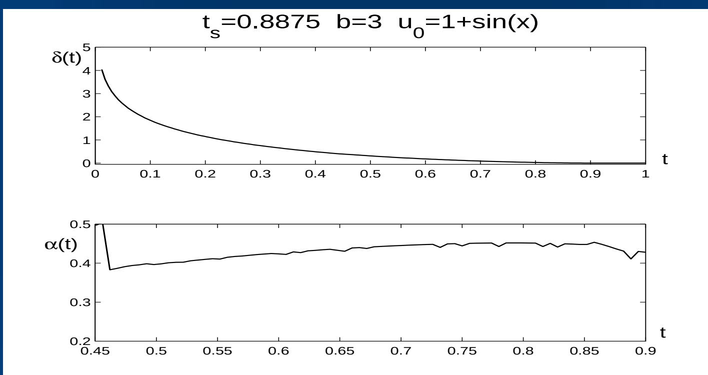

The singularity times and the type of singularities for differents values of b.

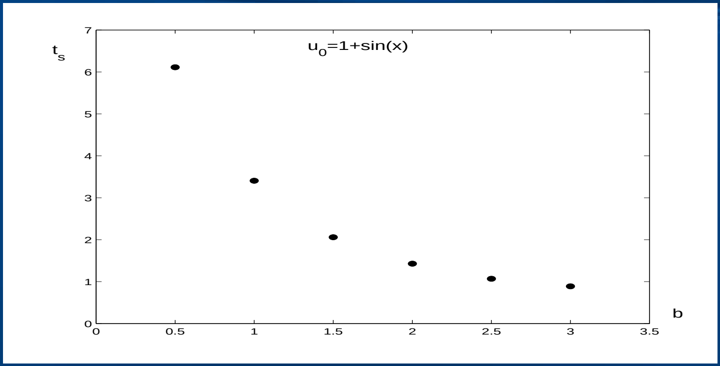

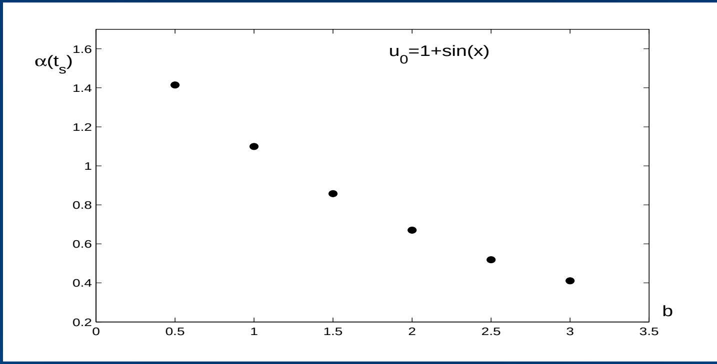

2. Zero viscosity limit for NS equations

Consider the Navier-Stokes equations:

$$\begin{aligned} \partial_t \boldsymbol{u} + (\boldsymbol{u} \cdot \boldsymbol{\nabla})\, \boldsymbol{u} + \boldsymbol{\nabla} p &= \nu \Delta\, \boldsymbol{u} \,, \\ \boldsymbol{\nabla} \cdot \boldsymbol{u} &= 0 \,, \\ \boldsymbol{u}(t=0) &= \boldsymbol{u}_0 \,, \end{aligned}$$

We want to consider the situation when the viscosity $\nu \longrightarrow 0$.

Formally one has that the solution should behave as prescribed by Euler equations.

$$\begin{aligned} \partial_t \boldsymbol{u} + \boldsymbol{u} \cdot \boldsymbol{\nabla} \boldsymbol{u} + \boldsymbol{\nabla} p &= 0 \\ \boldsymbol{\nabla} \cdot \boldsymbol{u} &= 0 \end{aligned}$$

This was proved by Swann Trans AMS 1971 in $\mathbb{R}^3$ (no boundaries) and by Constantin and Wu Nonlinearity 1995 for vortex patches in $\mathbb{R}^2$, i.e. when the initial vorticity is the characteristic function of a domain. The rate of convergence was $O(\nu)$.

2. Zero viscosity limit for NS equations

Consider the Navier-Stokes equations:

$$\begin{aligned} \partial_t \boldsymbol{u} + (\boldsymbol{u} \cdot \boldsymbol{\nabla})\, \boldsymbol{u} + \boldsymbol{\nabla} p &= \nu \Delta\, \boldsymbol{u}\ , \\ \boldsymbol{\nabla} \cdot \boldsymbol{u} &= 0\ , \\ \boldsymbol{u}(t=0) &= \boldsymbol{u}_0\ , \end{aligned}$$

We want to consider the situation when the viscosity $\nu \longrightarrow 0$.

Formally one has that the solution should behave as prescribed by Euler equations.

$$\begin{aligned} \partial_t \boldsymbol{u} + \boldsymbol{u} \cdot \boldsymbol{\nabla} \boldsymbol{u} + \boldsymbol{\nabla} p &= 0 \\ \boldsymbol{\nabla} \cdot \boldsymbol{u} &= 0 \end{aligned}$$

This was proved by Swann Trans AMS 1971 in $\mathbb{R}^3$ (no boundaries) and by Constantin and Wu Nonlinearity 1995 for vortex patches in $\mathbb{R}^2$, i.e. when the initial vorticity is the characteristic function of a domain. The rate of convergence was $O(\nu)$.

We want to discuss a different situation:

- Fluids with boundaries, e.g. half–plane, half–space, exterior of a disk.

Fluids in presence of a boundary

The discrepancy between the boundary conditions $\mathbf{u} = \mathbf{0}$ for NS and $u_n = 0$ for Euler, makes it clear that one cannot hope:

$$\left\| \boldsymbol{u}^{NS} - \boldsymbol{u}^{E} \right\| \longrightarrow 0 \qquad \text{when} \quad \sqrt{\nu} = \varepsilon \to 0 \ ,$$

at least close to the boundary.

Fluids in presence of a boundary

The discrepancy between the boundary conditions $\mathbf{u} = \mathbf{0}$ for NS and $u_n = 0$ for Euler, makes it clear that one cannot hope:

$$\left\| \boldsymbol{u}^{NS} - \boldsymbol{u}^{E} \right\| \longrightarrow 0 \qquad \text{when} \quad \sqrt{\nu} = \varepsilon \to 0 \ ,$$

at least close to the boundary.

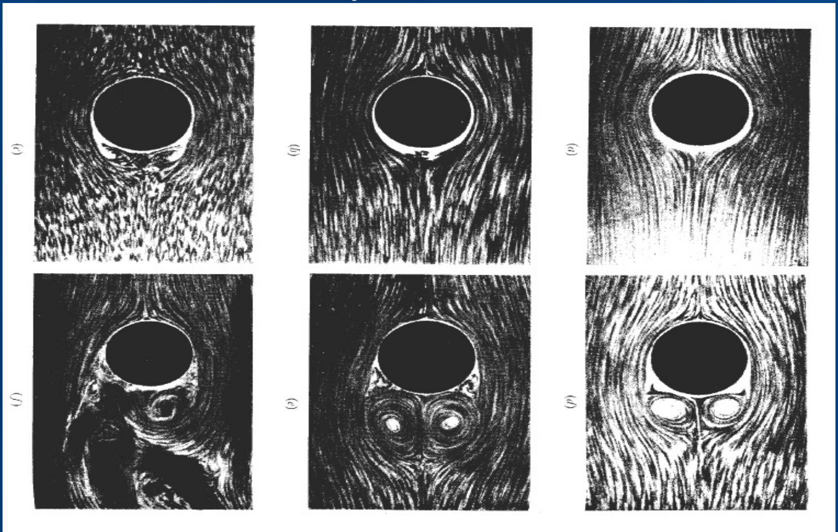

The above picture is in contrast with conservation of vorticity unless a huge amount of voricity is created at the boundary.

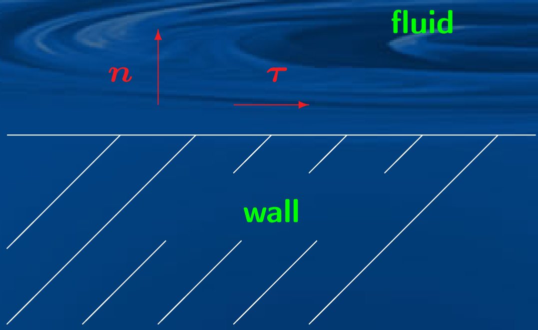

When $\nu \to 0$ one gets a singular limit.
The fluid shows two different regimes.

- Far away from the boundary:
  viscous forces $\ll$ *inertial forces* $\Longrightarrow$ Euler equations might be OK

- Close to the boundary:
  viscous forces are NOT neglegible $\Longrightarrow$?? equations?
  Something wild is going on close to the boundary: high generation of vorticity.

The desire to get a simplification led Prandtl to use asymptotics.
His procedure is based on the following ideas:

- Away from the boundary viscous forces ($\varepsilon^2 \Delta \boldsymbol{u}$) can be neglected wrt convective forces ($\boldsymbol{u} \cdot \nabla \boldsymbol{u}$). Euler OK.
- Close to the boundary viscous forces stop the fluid. They cannot be neglected.
- The transition between the two regimes is rapid.

  This is implemented through the scaling, valid close to the boundary:

$$Y = y/\varepsilon \qquad \text{and hypothesis} \quad \partial_Y u = O(1) \ .$$

- Moreover $\partial_x u = O(1)$.

This implies: $\varepsilon^2 \partial_{yy} u = \partial_{YY} u = O(1) = u \partial_x u$.

The desire to get a simplification led Prandtl to use asymptotics.
His procedure is based on the following ideas:

- Away from the boundary viscous forces ($\varepsilon^2 \Delta \boldsymbol{u}$) can be neglected wrt convective forces ($\boldsymbol{u} \cdot \nabla \boldsymbol{u}$). Euler OK.
- Close to the boundary viscous forces stop the fluid. They cannot be neglected.
- The transition between the two regimes is rapid.

  This is implemented through the scaling, valid close to the boundary:

$$Y = y/\varepsilon \qquad \text{and hypothesis} \quad \partial_Y u = O(1) \ .$$

- Moreover $\partial_x u = O(1)$.

This implies: $\varepsilon^2 \partial_{yy} u = \partial_{YY} u = O(1) = u \partial_x u$.
Introducing the above scaling in the NS equations:

$$\begin{array}{rcl}
\partial_t u + u\partial_x u + v\partial_Y u + \partial_x p & = & \partial_{YY} u \\
\partial_Y p & = & 0 \\
\partial_x u + \partial_Y v & = & 0 \\
u(x, Y = 0) = v(x, Y = 0) & = & 0 \\
u(x, Y \to \infty) & \longrightarrow & u^E(x, y = 0) \\
u(x, y, t = 0) & = & u_{in} \ .
\end{array}$$

The procedure is therefore:
First solve Euler equations. Get the boundary data $u^E(y = 0)$
Then solve Prandtl with the matching condition.

Relevance of Prandtl's equations

- Prandtl's equations, in their essence, look particularly simple: they just are one equation for the tangential velocity u:

$$\partial_t u + u\partial_x u + v\partial_Y u + \partial_x p^E = \partial_{YY} u$$

Therefore they are a good toy model to mimic the particularly complicated behavior (generation of vorticity) of the NS solutions near the boundary.

They have been successfully used to calculate quantities of practical importance like drag coefficient, or shear stress.

- A fundamental problem in fluid dynamics is to prove that $u^{NS} \to u^E$ away from boundaries.

Kato in 1984 proved his famous criterion:

Theorem

The following conditions are equivalent:

$$\|\boldsymbol{u}^{NS} - \boldsymbol{u}^E\|_{L^2} \longrightarrow 0 \quad \text{uniformly in } t \in [0, T] \tag{2}$$

$$\nu \int_0^T \|\boldsymbol{\nabla u}^{NS}\|^2_{\Gamma_\nu} dt \longrightarrow 0. \tag{3}$$

Where $\|\cdot\|_{\Gamma_\nu}$ denotes the L^2-norm restricted to a strip of width $O(\nu)$ close to the boundary.

If one wants to solve the zero viscosity problem of the NS equations one has to face the boundary layer:
i.e. control or improve (or disprove) Prandtl's equations.

Well posedness results

- Short time existence if the initial data are monotonous (no initial shear layer).
  This is the Oleinik '67 result.

- Long time existence if one adds the hypothesis that the outer pressure gradient is favourable,i.e. $\partial_x p = -U\partial_x U \leq 0$. This means that no mechanism that can produce shear layer is present.
  This is Xin and Zhang '03 result.

- Short time existence for analytic data (without assuming monotonicity). This means that the data are highly non turbulent. Higher Fourier modes are almost non existent.
  Sammartino and Caflisch '98
  Lombardo Cannone and Sammartino '03.

THE DARK SIDE OF PRANDTL's EQUATIONS

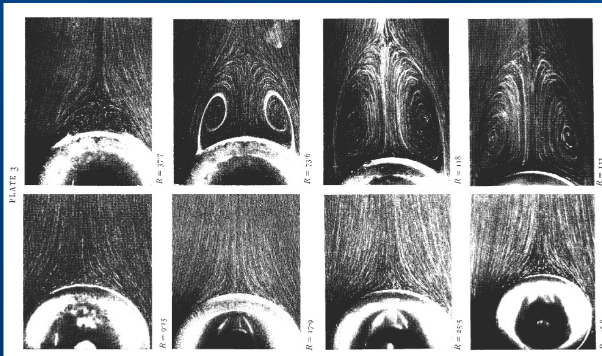

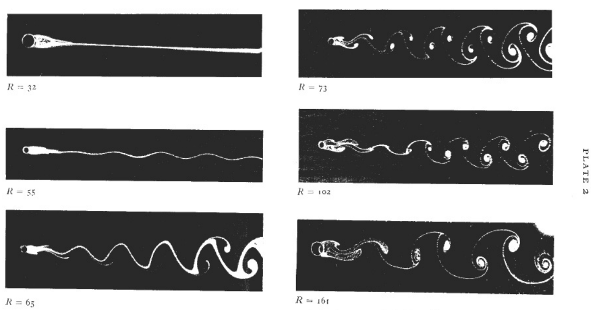

Figure 4.12.6. Streak lines in the wake behind a circular cylinder in a stream of oil. (From Homann 1936*a*.)

Vorticity is generated at the boundary.
The mechanism through this vorticity is shed into the main flow is separation, i.e. the detachment of the boundary layer.
SINGULARITY OF PRANDTL'S EQUATIONS.

The possibility that the unsteady Prandtl's equations developed singularity was:

- conjectured in the '60s.
- First disproved (numerically with low resolution) in the '70s.
- Found numerically in the '80s by Van Dommelen and Shen in the case of the impulsively started disk.

The Van Dommelen and Shen's singularity is a shock and is ubiquitous.

In fact was also found for other boundary layer flows, like cavity flow (E and Liu '96) and thick core vortex flow Cassel '00, Obabko and Cassel '02,'05.

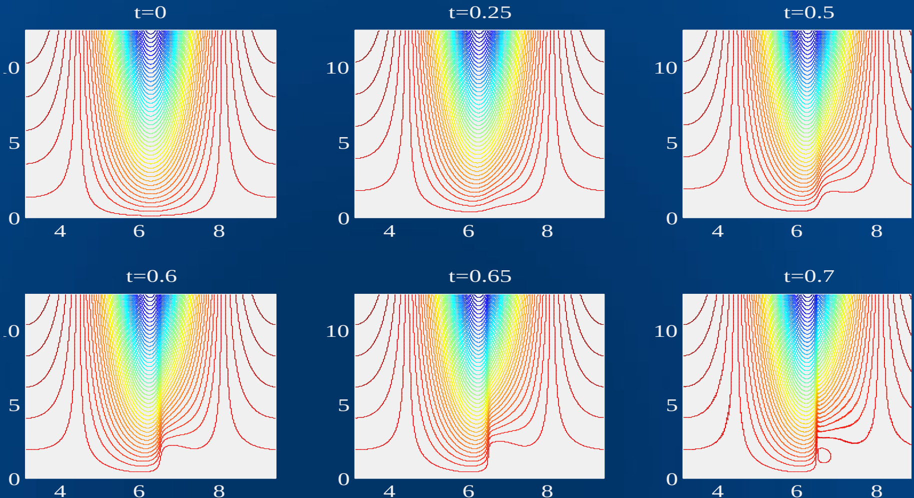

The physical mechanisms that lead to the VDS singularity is recirculation:

- It forms back-flow, and a stagnation point, as the result of adverse pressure gradient;
- Then two counter rotating vortices appear;
- Growth of these vortices;
- Finally, a singularity with eruption of fluid from within the boundary layer: separation.

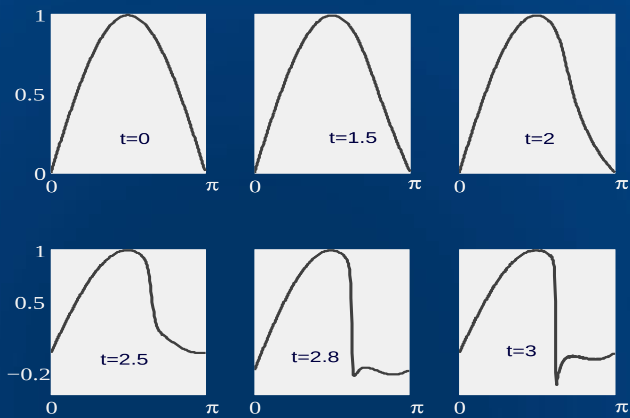

The physical mechanisms that lead to the VDS singularity is recirculation:

- It forms back-flow, and a stagnation point, as the result of adverse pressure gradient;
- Then two counter rotating vortices appear;
- Growth of these vortices;
- Finally, a singularity with eruption of fluid from within the boundary layer: separation.

Complex Singularity Tracking and Separation Singularity

In Della Rocca, Lombardo, Sammartino, S.'05 it is studied the VDS singularity using the singularity tracking method.
It is possible to extend the technique of tracking singularity for bi–dimensional functions.

Complex Singularity Tracking and Separation Singularity

In Della Rocca, Lombardo, Sammartino, S.'05 it is studied the VDS singularity using the singularity tracking method.
It is possible to extend the technique of tracking singularity for bi–dimensional functions.
A first way (Frisch et al. '05) consists to applying the technique of tracking singularity to the shell–summed amplitude of the Fourier expansion. Given a function $u(z, w)$, with z and w complex variables, with

$$u(z, w) = \sum_{h,k} a_{hk} e^{ihz} e^{ikw},$$

the corresponding shell–summed Fourier amplitude is defined by

$$A_K \equiv \sum_{K \leq |\kappa| < K+1} a_{hk},$$

where $|\kappa| = |(h, k)|$. At this point one can evaluate by Laplace asymptotic formula with the behavior of A_K determining the distance δ of the singularity and its algebraic characterization, like in the one dimensional case.

Another possible extension (Poincaré 1899, Tsikh 1993) consists to evaluate the Laplace asymptotic formula for each direction of the fourier spectrum and the distance δ is the minimum over all directions.

Another possible extension (Poincaré 1899, Tsikh 1993) consists to evaluate the Laplace asymptotic formula for each direction of the fourier spectrum and the distance δ is the minimum over all directions.

Consider $\vec{k} = (k\cos(\theta), k\sin(\theta))$.

$$\begin{aligned}\widehat{u}_{\vec{k}} &= \int\int u(x,y)e^{-i\vec{k}\cdot\vec{x}}d\vec{x} \\ &= \int \left(\int u(x_{\parallel}\widehat{k} + x_{\perp}\widehat{k}_{\perp})dx_{\perp}\right) e^{-ikx_{\parallel}}dx_{\parallel} \\ &= \int g(x_{\parallel})e^{-ikx_{\parallel}}dx_{\parallel}.\end{aligned}$$

It follows from Laplace asymptotic formula that, for $k \longrightarrow \infty$, $\widehat{u}_{\vec{k}} \sim e^{-ikx^*_{\parallel}}$, where $x^*_{\parallel}$ is the singularity of $g(x_{\parallel})$ in the complex $x_{\parallel}$ plane nearest to the real domain. Hence $|\widehat{u}_{\vec{k}}| \sim e^{-\delta(\theta)}$ where $\delta(\theta) = -\Im x^*_{\parallel}$.

Another possible extension (Poincaré 1899, Tsikh 1993) consists to evaluate the Laplace asymptotic formula for each direction of the fourier spectrum and the distance δ is the minimum over all directions.

Consider $\vec{k} = (k\cos(\theta), k\sin(\theta))$.

$$
\begin{aligned}
\widehat{u}_{\vec{k}} &= \int\int u(x,y)e^{-i\vec{k}\cdot\vec{x}}d\vec{x} \\
&= \int\left(\int u(x_{\parallel}\widehat{k} + x_{\perp}\widehat{k}_{\perp})dx_{\perp}\right)e^{-ikx_{\parallel}}dx_{\parallel} \\
&= \int g(x_{\parallel})e^{-ikx_{\parallel}}dx_{\parallel}.
\end{aligned}
$$

It follows from Laplace asymptotic formula that, for $k \longrightarrow \infty$, $\widehat{u}_{\vec{k}} \sim e^{-ikx_{\parallel}^*}$, where $x_{\parallel}^*$ is the singularity of $g(x_{\parallel})$ in the complex $x_{\parallel}$ plane nearest to the real domain. Hence $|\widehat{u}_{\vec{k}}| \sim e^{-\delta(\theta)}$ where $\delta(\theta) = -\Im x_{\parallel}^*$.

To solve numerically Prandtl's equations we use the mixed spectral Fourier-Chebyshev numerical scheme

$$
u(x,Y,\triangle t) \approx \sum_{k=-K/2}^{k=K/2}\sum_{j=0}^{j=M} u_{k,j}^n e^{ikx}T_j(Y)
$$

The temporal scheme used is the two step RK–CN to treat implicitly the diffusive term.
The normal velocity component is recovered by numerical integration through the incompressibility condition.

The profile of the distance δ at the singularity time w.r.t. the angle θ for the solution of Prandtl's equation in the VDS case. The distance δ is an increase function of θ, with $\approx 10^{-4}$ when $\theta \approx 0.035\pi$.

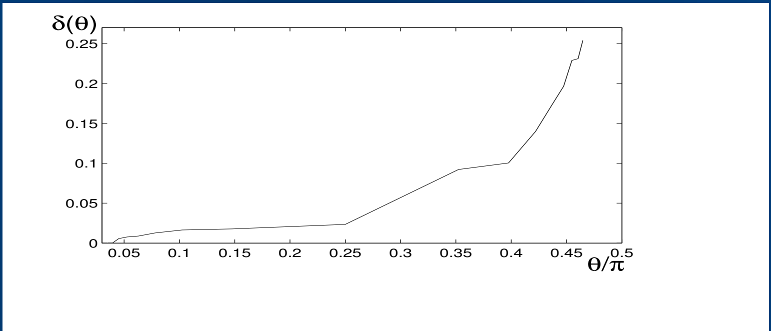

Thus for the VDS initial condition, one can studies the singularity formation of Prandtl applying the singularity tracking method to the x variable at different values of the normal Y variable. The distance reaches its minimum at location $Y \approx 5$.

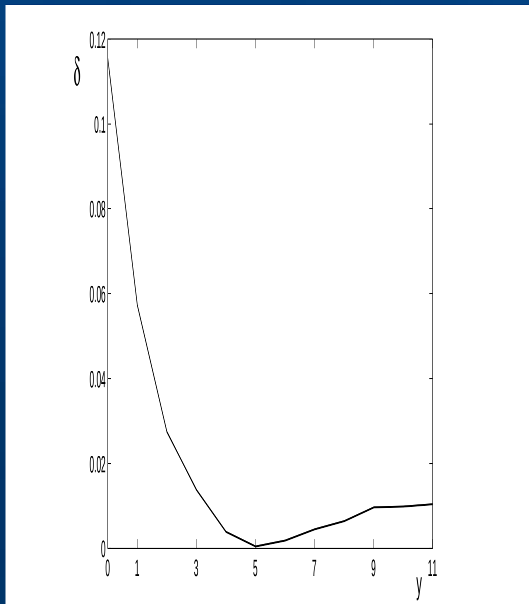

Therefore, an estimation on the rate of the exponential decay δ of the spectrum in the streamwise variable at location $Y = 5$, gives the distance of the VDS singularity from the real axes, and the first time t_s at which $\delta(t_s) = 0$ gives the exact time of the development of the singularity.

A shock type singularity $\alpha \approx 1/3$ forms at time $t_s \approx 3$ at location $x^* \approx 1.95$ and $Y \approx 5$.

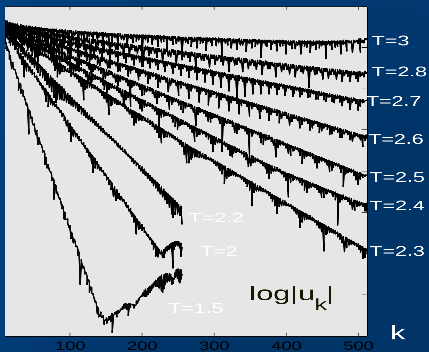

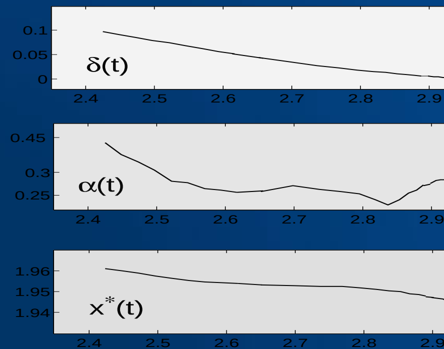

Prandtl and NS: Row of equidistant point vortices

In a cartesian frame, the vortices are centered in $(ma+\pi, b)_{m\epsilon\in\mathbb{Z}}$, where b is the distance of the the row from the wall and a is the distance of two consecutive vortices.
Each vortex moves with uniform velocity $U = \frac{k}{2a}\coth(\frac{2\pi b}{a})$ parallel to the wall.

$$\Psi(x,y) = Uy - \frac{k}{4\pi}\log\frac{\cosh(\frac{2\pi}{a}(y-b)) - \cos(\frac{2\pi}{a}(x-\pi))}{\cosh(\frac{2\pi}{a}(y+b)) - \cos(\frac{2\pi}{a}(x-\pi))}.$$

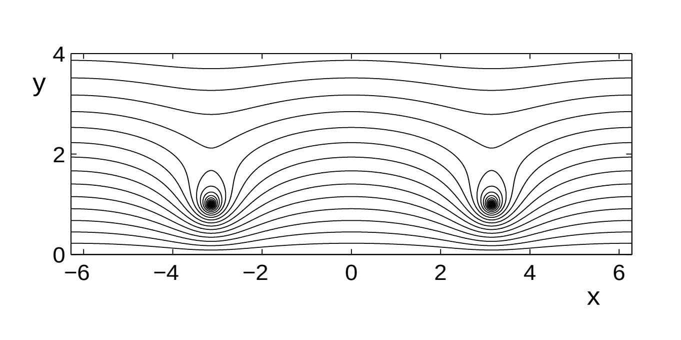

This is an a-periodic datum, and the velocity components obtained are such that $u = k/a$, $v = 0$ for $y = 0$, and $u, v \longrightarrow 0$ for $y \rightarrow \pm\infty$.
The initial vorticity is singular $w_0 = \sum_{m\in Z} \delta_{ma,b}$, where $\delta_{x,y}$ is Dirac's mass.
For NS, we approximate the initial vorticity with a finite sum of vortex blobs.

Tracking a . . .
Zero viscosity . . .
Pade . . .
Home Page
Title Page
Page 40 of 58
Go Back
Full Screen
Close
Quit

Prandtl's results

We use the singularity tracking method to trace the singularity in complex plane, obtaining that singularity forms at time $t_s \approx 0.74$ at location $x^* \approx 3.15$ and $Y \approx 2$. In (a) the time evolution of exponential decay of Fourier modes is shown. At $t \approx 0.74$, δ vanishes and a blow up for the first streamwise derivative occurs (b) in the profile of velocity u at $Y = 2$.

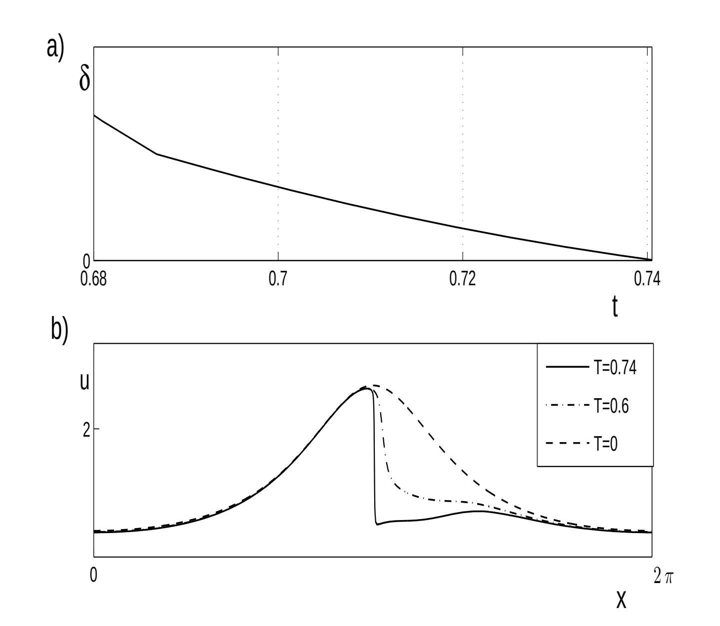

Streamline from Prandtl's calculations are shown. In Fig.(a) a recirculating eddy is formed and is grown in both streamwise and normal length (Fig.(b)). At $t = 0.67$ a kink seems to be formed in streamlines (Fig.(c)) and thickens in streamwise direction, evolving in a sharp spike at singularity time (Fig.(d)).

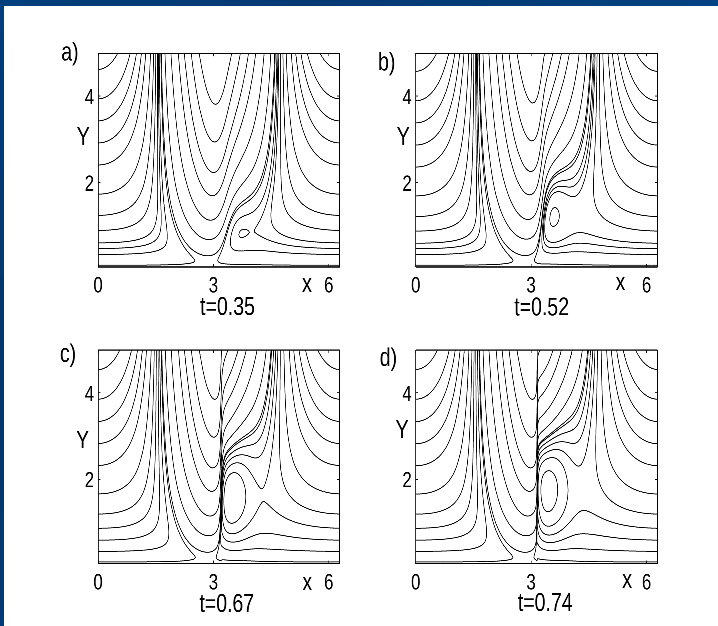

Navier Stokes results Re=10^4

a) and b) the streamlines, c) and d) the streamwise pressure gradient along the surface

$$\partial_x p_w = -\frac{1}{Re}\Gamma_y(\bar{y})\frac{\partial \omega}{\partial y}|_{y=0},$$

and the scaled skin friction coefficient (dashed) $C_f = -2\omega_{y=0}/Re$.

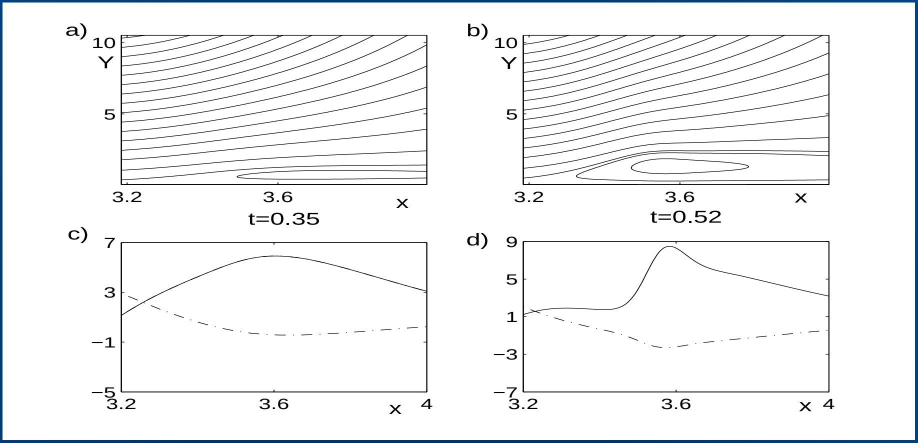

At time $t = 0.35$ the recirculation region is formed.
At time $t = 0.52$ it is visible the formation of a local minimum in the $\partial_x p_w$ in correspondence to the formation of a small spike in the recirculation region.

Navier Stokes results Re=10^4

a) and b) the streamlines, c) and d) the streamwise pressure gradient along the surface

$$\partial_x p_w = -\frac{1}{Re}\Gamma_y(\bar{y})\frac{\partial \omega}{\partial y}|_{y=0},$$

and the scaled skin friction coefficient (dashed) $C_f = -2\omega_{y=0}/Re$.

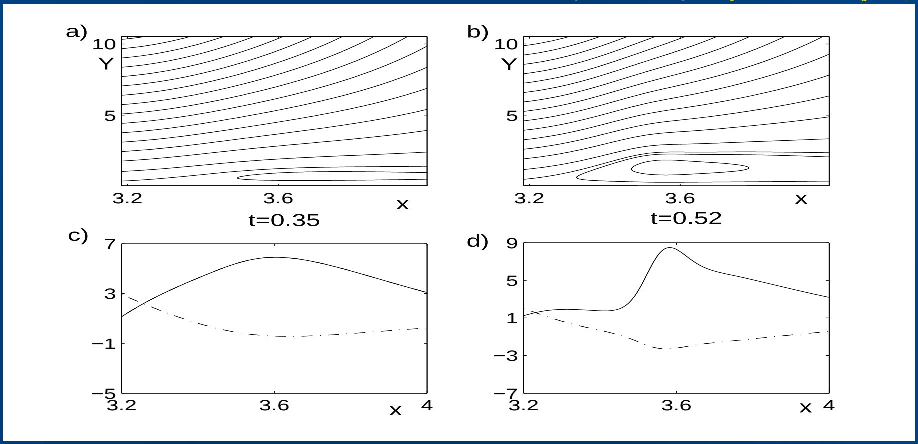

At time $t = 0.35$ the recirculation region is formed.
At time $t = 0.52$ it is visible the formation of a local minimum in the $\partial_x p_w$ in correspondence to the formation of a small spike in the recirculation region.

The formation of a minimum after the maximum position in $\partial_x p_w$ accelerates the formation of the spike: the flow across the boundary is compressed in the streamwise direction and this compression leads the recirculation region growth in the normal direction.

a) and b) The streamlines, c) and d) the streamwise pressure gradient at the wall and the skin friction coefficient (dashed) for Navier Stokes solution with $Re = 10^4$.

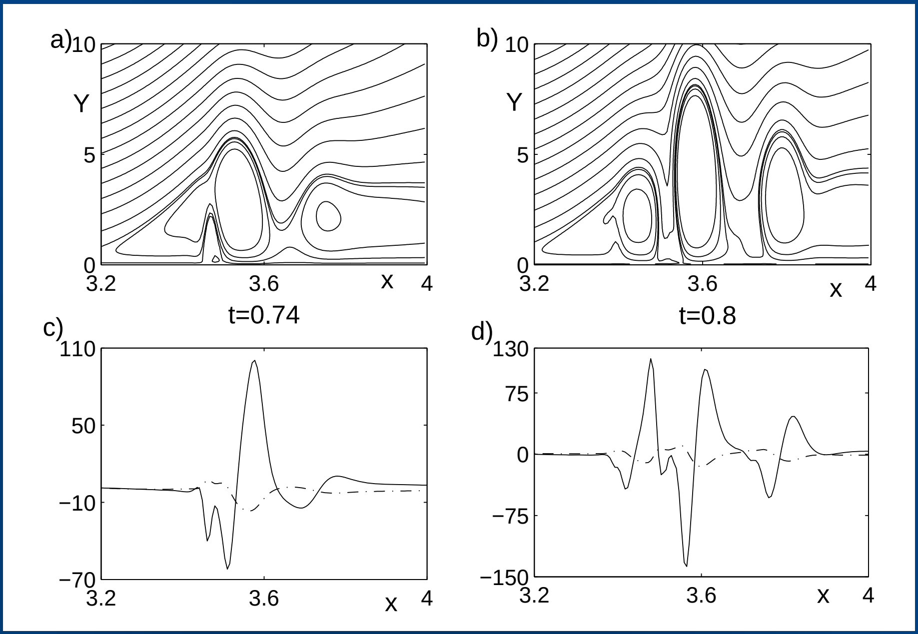

At time $t = 0.74$, the recirculation region has split into a series of corotating eddies in correspondence to the local maxima of streamwise pressure gradient.
The presence of more recirculating regions becomes more evident at time $t = 0.8$.

a) and b) The streamlines, c) and d) the streamwise pressure gradient at the wall and the scaled skin friction coefficient $10{*}C_f$ (dashed) for Navier Stokes solution at times $t = 0.74$ and $t = 0.8$.

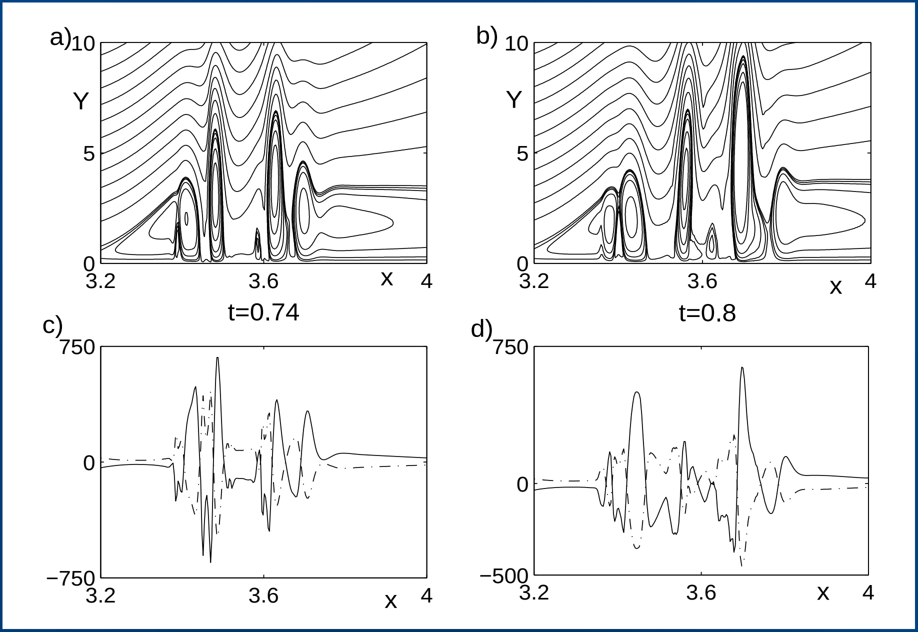

One can see the presence of a series (more) of corotating eddies as in the case of $Re = 5 * 10^4$.
The streamwise pressure gradient at the wall shows a more dramatic behavior with the presence of more pronounced spikes.

There is no spike formation on the upstream side of the recirculation region. Moreover the recirculation region does not split, and no other recirculation region exists close to the singularity time (Re=10^3).

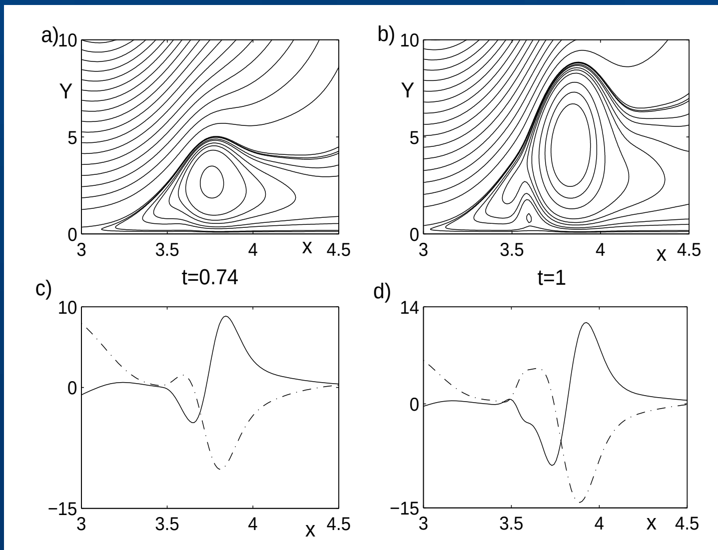

In (a) it is visible only one large recirculating eddy which splits at later time $t = 1$, where a second recirculating region is visible (b).
In (c)-(d) there is no evidence of forming spike as in the case of the moderate-high Re numbers.

Comparison

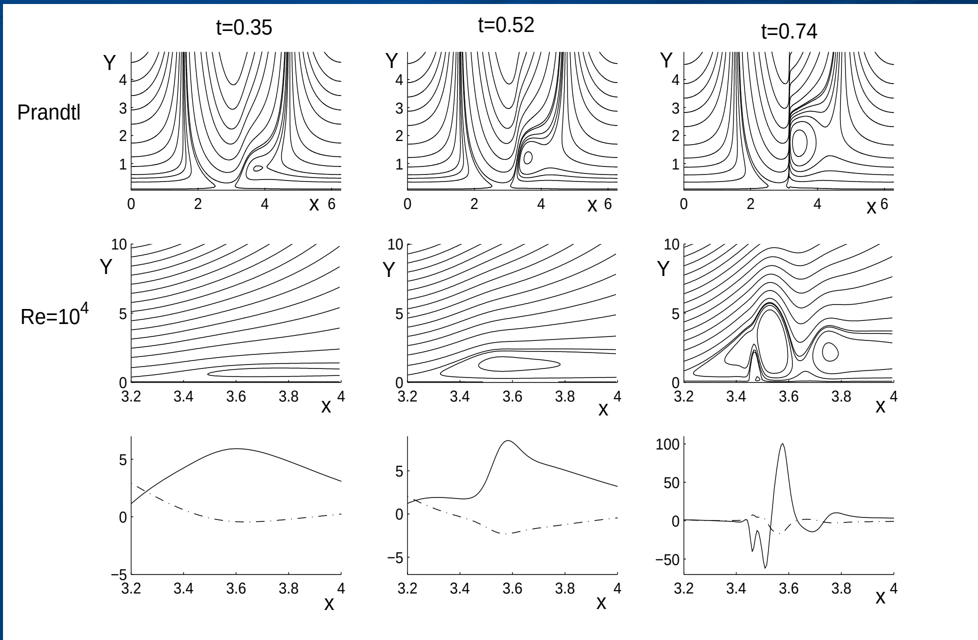

Viscous–inviscid (large–scale) interaction is quite early with respect to theoretical prediction of boundary layer. A kink is visible at $t \approx 0.52$, with increasing streamwise thickness as Re decreases. This evolves in a spike for $Re = 10^4 - 5 \cdot 10^4$ as in the boundary layer results.

At this stage a new type of (small-scale) interaction is visible. For $Re = 10^4 - Re = 5 \cdot 10^4$ the recirculation region is splitting and one can see the formation of a secondary spikes at $t \approx 0.74$.

The evolution in time of $\partial_x p_w$, starting at $t = 0.1$ with increments of 0.1.

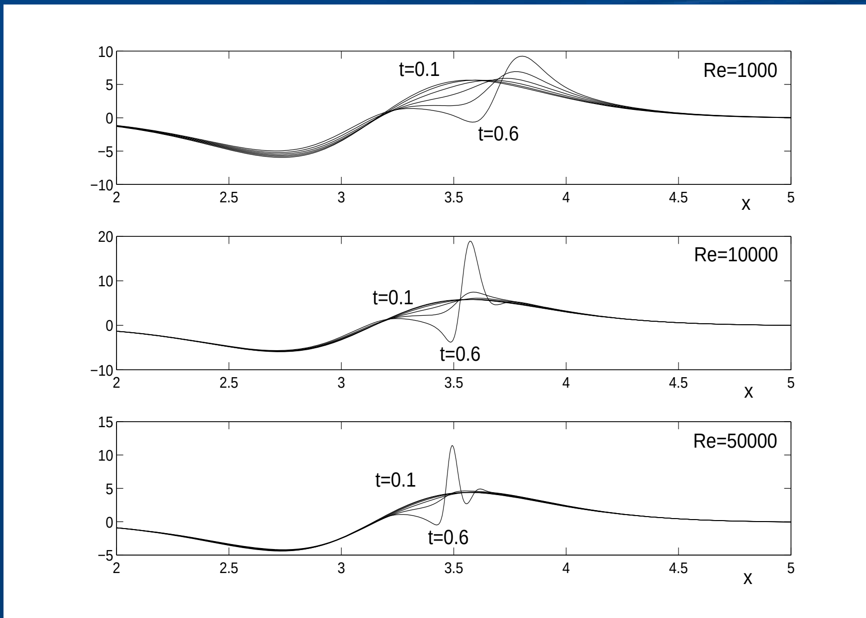

For $Re = 10^3$ the streamwise pressure gradient remains the same essentially up to $t \approx 0.2$ while for $Re = 10^4 - 5 \cdot 10^4$ the interaction seems to start later at $t \approx 0.3$. Re number increases the interaction begins later.

The evolution in time of $\partial_x p_w$, starting at $t = 0.1$ with increments of 0.1.

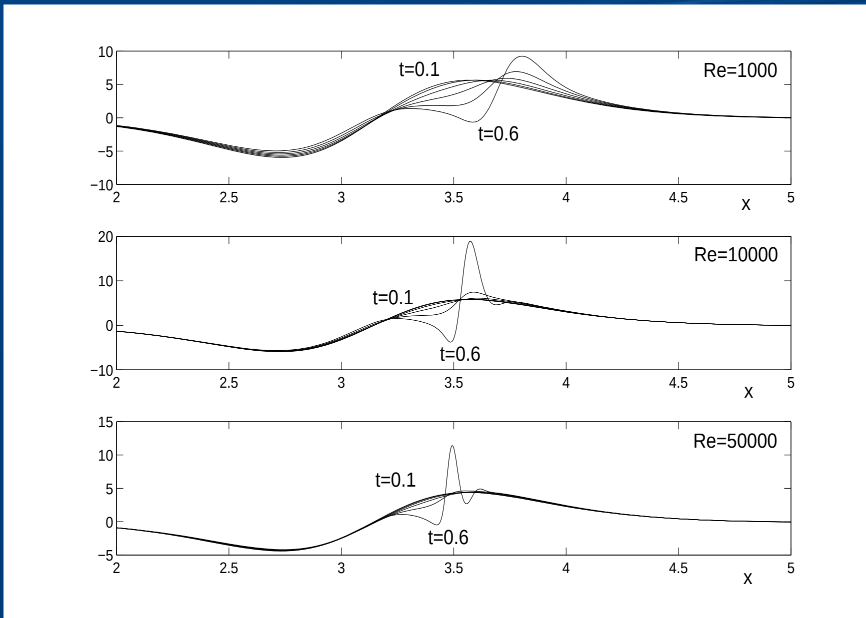

For $Re = 10^3$ the streamwise pressure gradient remains the same essentially up to $t \approx 0.2$ while for $Re = 10^4 - 5 \cdot 10^4$ the
interaction seems to start later at $t \approx 0.3$. Re number increases the interaction begins later.

For $Re = 10^3$ there is only one recirculation region close to singularity time, as in boundary layer solution, but in this case no spike and no small–scale interaction exists.

The evolution in time of L_∞ norm of the normal pressure gradient at the wall for Navier Stokes solutions with different Re numbers. For $Re = 10^3$ the variation is more pronounced at early time cause the viscous-inviscid interaction. At later time a rapidly growth occurs cause the formation of a small-scale interaction for $Re = 10^4, 5 \cdot 10^5$.

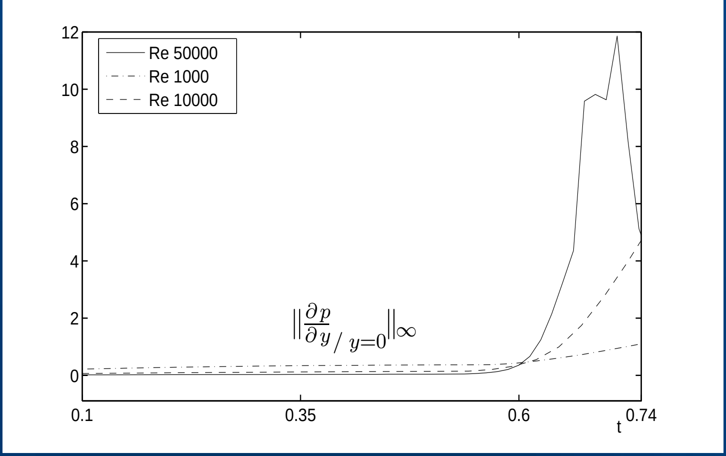

The evolution in time of L_∞ norm of the normal pressure gradient at the wall for Navier Stokes solutions with different Re numbers. For $Re = 10^3$ the variation is more pronounced at early time cause the viscous-inviscid interaction. At later time a rapidly growth occurs cause the formation of a small-scale interaction for $Re = 10^4, 5 \cdot 10^5$.

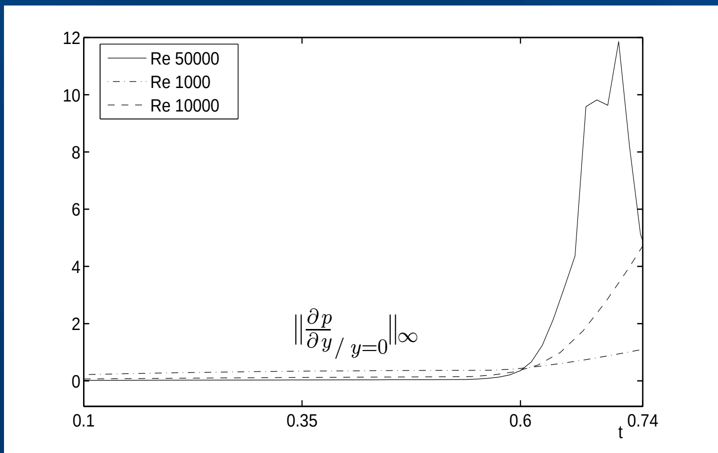

Lower Re numbers (as 10^3) characterized by a large–scale interaction acting over the flow: no spike-like behavior in the solution.

Moderate–high Re (10^4, $5 \cdot 10^4$) with a small-scale interaction at a time preceding the formation of singularity in boundary layer solution.

High Re: no large–scale interaction and the small-scale interaction acts at a time close to singularity time.

Analysis of singularities for NS (VDS initial datum)

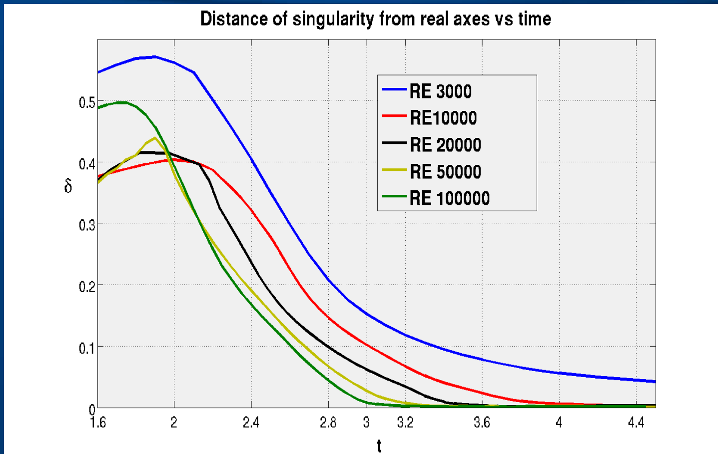

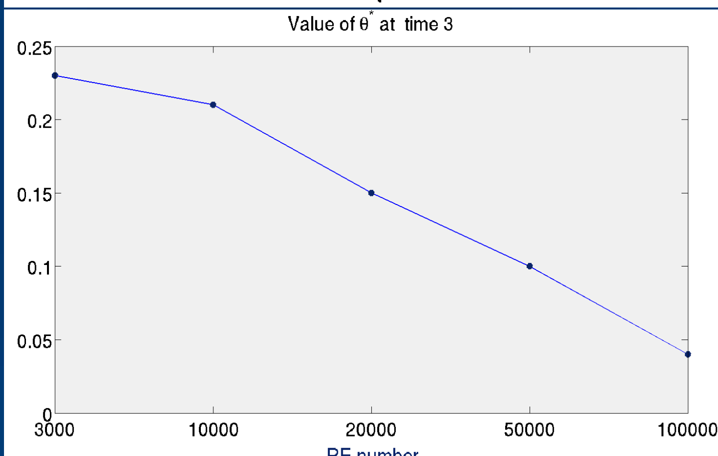

Padé Approximant

Consider the power series $f(Z) = \sum_{k=0}^{\infty} c_k Z^k$, the [L,M] Padé Approximant to this series is defined as the rational function

$$P_{[L,M]} = \frac{a_0 + a_1 Z + \cdots + a_L Z^L}{1 + b_1 Z + \cdots + b_M Z^M},$$

with the property that:

$$f(Z) - P_{[L,M]} = O\left(Z^{L+M+1}\right).$$

Here we shall use only approximants with $L = M$.

Padé Approximant

Consider the power series $f(Z) = \sum_{k=0}^{\infty} c_k Z^k$, the [L,M] Padé Approximant to this series is defined as the rational function

$$P_{[L,M]} = \frac{a_0 + a_1 Z + \cdots + a_L Z^L}{1 + b_1 Z + \cdots + b_M Z^M},$$

with the property that:

$$f(Z) - P_{[L,M]} = O\left(Z^{L+M+1}\right).$$

Here we shall use only approximants with $L = M$.

The same idea may be applied to Fourier series with $Z = e^{-ix}$:

$$u(x) \simeq \sum_{k=-N}^{N} \hat{u}_k e^{-ikx} = P_{[L,M]} + Q_{[L,M]} - \hat{u}_0,$$

where

$$\sum_{k=0}^{N} \hat{u}_k e^{-ikx} = P_{[\frac{1}{2}N,\frac{1}{2}N]} + O\left(Z^{N+1}\right)$$

$$\sum_{k=-N}^{0} \hat{u}_k e^{-ikx} = Q_{[\frac{1}{2}N,\frac{1}{2}N]} + O\left(Z^{N+1}\right).$$

Analysis of singularities for NS (VDS initial datum)

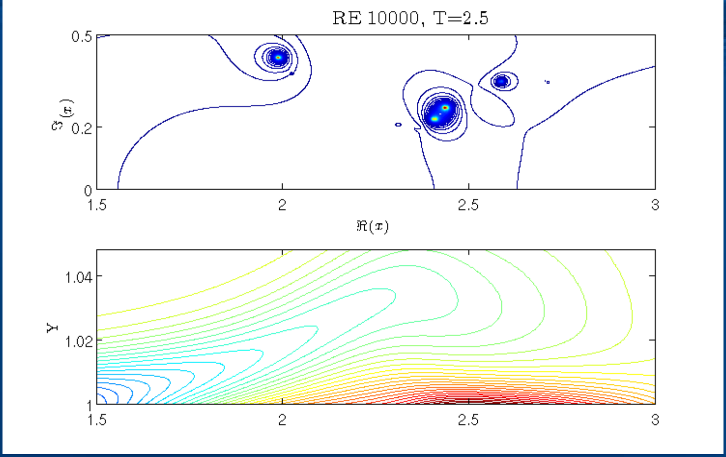

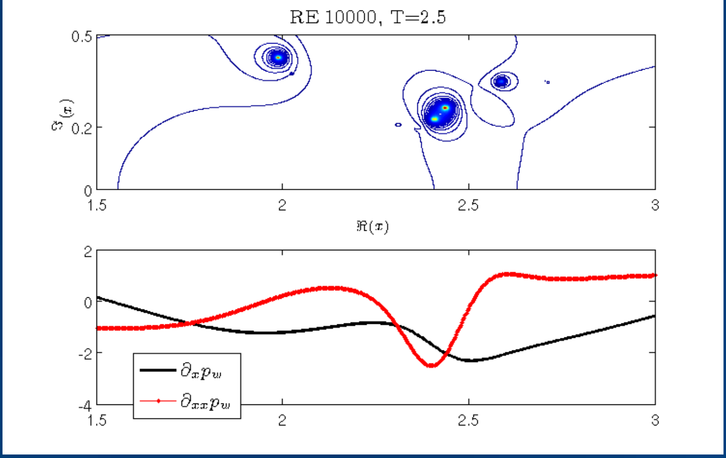

Analysis of singularities for NS (VDS initial datum)

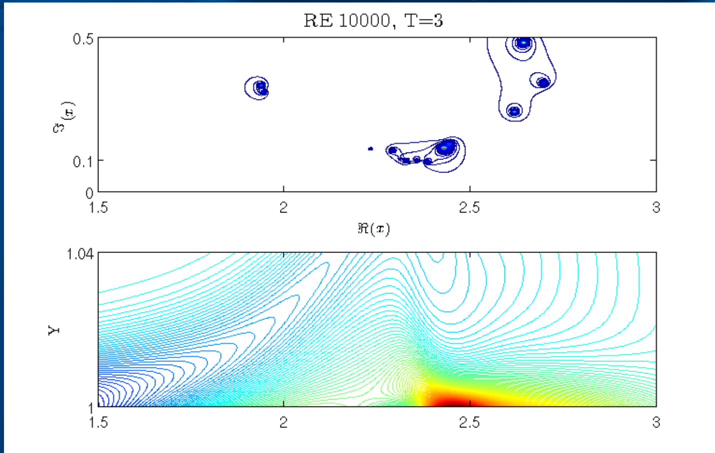

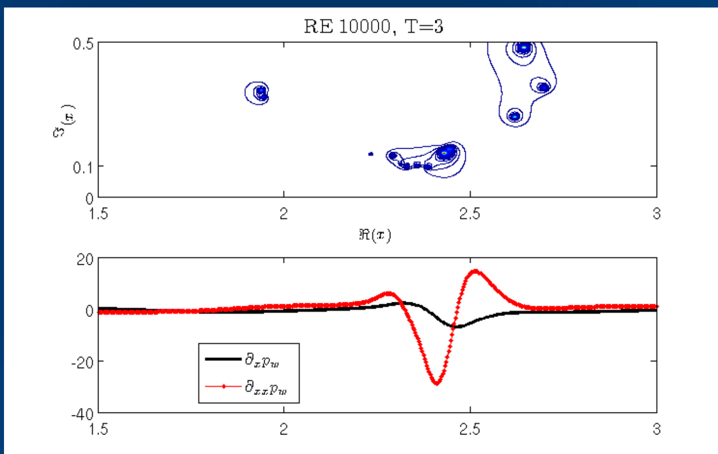

Tracking a . . .
Zero viscosity . . .
Pade . . .
Home Page
Title Page
Page 53 of 58
Go Back
Full Screen
Close
Quit

Analysis of singularities for NS (VDS initial datum)

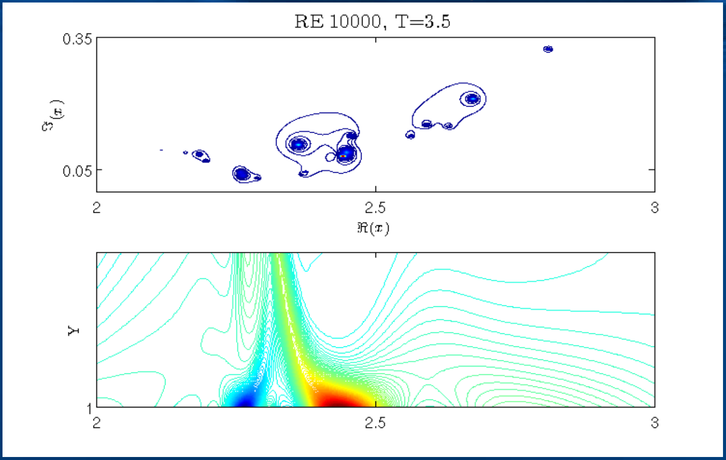

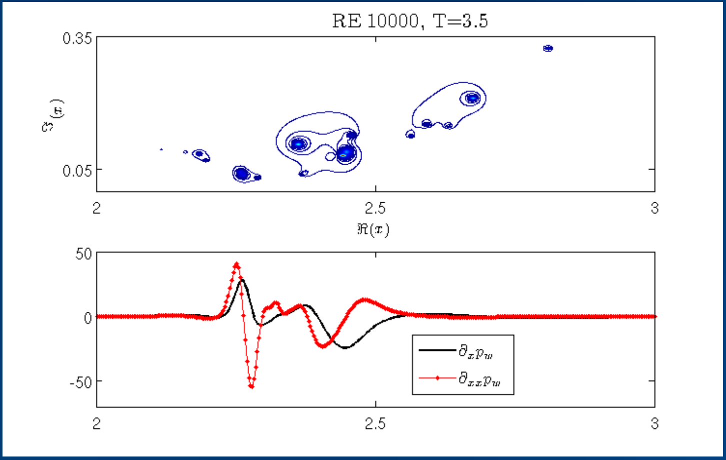

3. Pade Approximant: Viscous Burger's Equation

$$
\begin{aligned}
u_t + uu_x &= \nu u_{xx}, \qquad x \in [0, 2\pi] \\
u(x, t = 0) &= u_0(x) = \sin(x), \\
u(0, t) &= u(2\pi, t).
\end{aligned}
$$

3. Pade Approximant: Viscous Burger's Equation

$$
\begin{aligned}
u_t + u u_x &= \nu u_{xx}, \qquad x \in [0, 2\pi] \\
u(x, t=0) &= u_0(x) = \sin(x), \\
u(0, t) &= u(2\pi, t).
\end{aligned}
$$

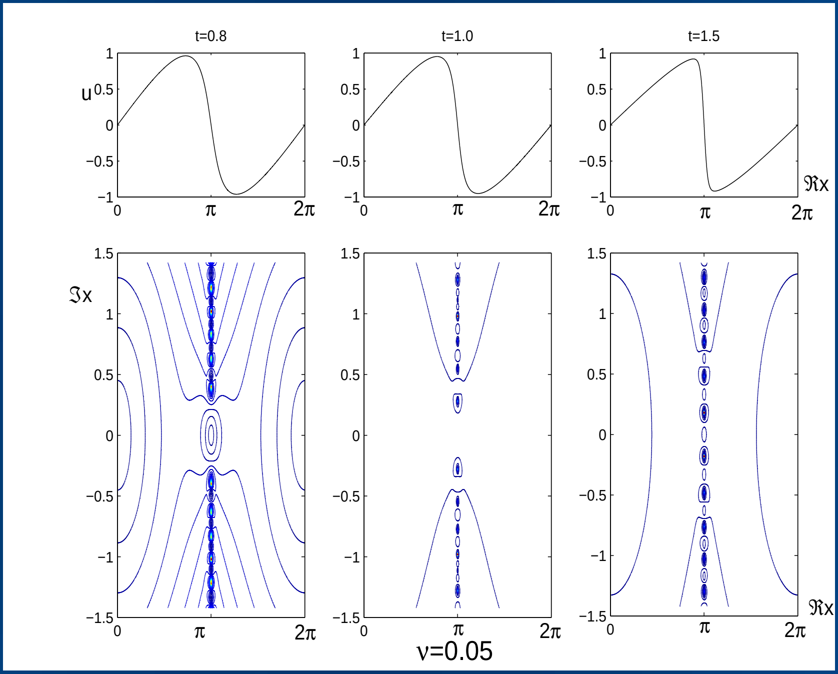

Pade Approximant: 'Dispersion' Burger's Equation

$$\begin{aligned} u_t + uu_x &= \epsilon e^{i\theta} u_{xx}, \qquad x \in [0, 2\pi] \\ u(x, t=0) &= u_0(x) = \sin(x), \\ u(0,t) &= u(2\pi, t). \end{aligned}$$

(Dobrokhotov et al 92 – Senouf, Caflisch and Ercolani 96)

Pade Approximant: 'Dispersion' Burger's Equation

$$\begin{aligned} u_t + uu_x &= \epsilon e^{i\theta} u_{xx}, \qquad x \in [0, 2\pi] \\ u(x, t=0) &= u_0(x) = \sin(x), \\ u(0,t) &= u(2\pi, t). \end{aligned}$$

(Dobrokhotov et al 92 – Senouf, Caflisch and Ercolani 96)

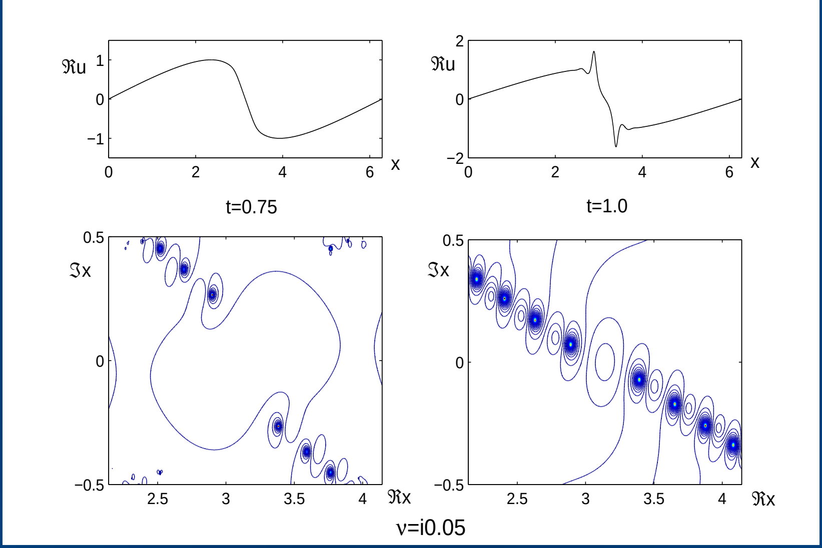

Pade Approximant: KdV equation

$$u_t + uu_x + \epsilon u_{xxx} = 0, \qquad x \in [0, 2\pi]$$
$$u(x, t = 0) = u_0(x) = \sin(x),$$
$$u(0, t) = u(2\pi, t).$$

Pade Approximant: KdV equation

$$u_t + uu_x + \epsilon u_{xxx} = 0, \qquad x \in [0, 2\pi]$$
$$u(x, t = 0) = u_0(x) = \sin(x),$$
$$u(0, t) = u(2\pi, t).$$

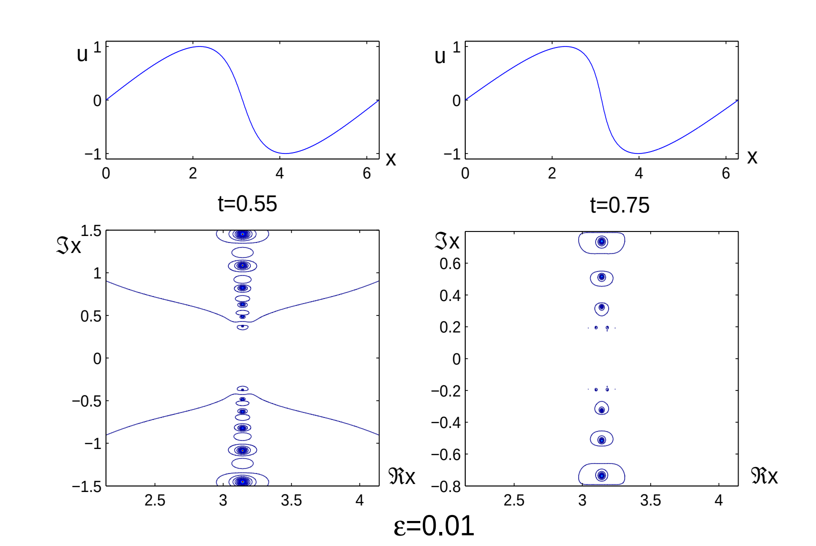

Pade Approximant: KdV equation

$$u_t + uu_x + \epsilon u_{xxx} = 0, \qquad x \in [0, 2\pi]$$
$$u(x, t = 0) = u_0(x) = \sin(x),$$
$$u(0, t) = u(2\pi, t).$$